Cellular Oncology 30 (2008) 337–347
DOI 10.3233/CLO-2008-0429
IOS Press

Altered cellular distribution and sub-cellular sorting of doppel (Dpl) protein in human astrocytoma cell lines

Elena Sbalchiero *, Alberto Azzalin *, Silvia Palumbo, Giulia Barbieri, Agustina Arias, Luca Simonelli, Luca Ferretti and Sergio Comincini **

Dipartimento di Genetica e Microbiologia, Università di Pavia, Pavia, Italy

Abstract. Doppel, a prion-like protein, is a GPI-membrane anchored protein generally not expressed in the Central Nervous System (CNS) of different mammalian species, including human. Nevertheless, in astrocytomas, a particular kind of glial tumors, the doppel encoding gene (*PRND*) is over-expressed and the corresponding protein product (Dpl) is ectopically localized in the cytoplasm of the tumor cells. In this study we have analysed the sub-cellular localization of Dpl using double-immunofluorescence staining and confocal microscopy examinations in two astrocytoma-derived human cell lines (IPDDC-A2 and D384-MG). Our results confirmed that Dpl is localized in the cytoplasm of the astrocytoma cells and indicated that it is mostly associated with Lamp-1 and Limp-2 positive lysosomal vesicles and, marginally, to the Golgi apparatus and other cellular organelles. Noticeably, none of the examined tumor cells showed a membrane-Dpl localization. The membrane-associated Dpl expression was restored after the transfection of the astrocytoma cells with mutated Dpl-expression vectors in its glycosylation sites. Additionally, Dpl showed altered expression and traffic using the acidotropic agent ammonium chloride, leading to the accumulation of Dpl in nascent exocytic vesicles. Altogether, these results indicated that in the astrocytic tumor cells Dpl has an altered biosynthetic trafficking, likely derived from abnormal post-translational processes: these modifications do not permit the localization of Dpl in correspondence of the plasma membrane and lead to its intracellular accumulation in the lysosomes. In these proteolytic compartments, the astrocytic tumor cells might provide to the degradation of the excess of a potentially cytotoxic Dpl product.

Keywords: Glioma, immunofluorescence, prion-like protein, lysosome

1. Introduction

The first prion paralogue gene, doppel, has been recently discovered [25], leading to the hypothesis that ancestral gene-duplication events might have originated a prion-related gene family [7]. On the course of evolution, functional divergences have contributed to the different expression profile patterns of the cellular prion (PrP^C) and doppel (Dpl) proteins, with the former widely expressed in different tissues, particularly in the CNS [23] and the latter localized mainly in the testicular tissue of different mammalian species [13, 34]. Additionally, functional divergence has related PrP^C to the occurence and propagation of prion diseases in humans and animals, as originally proposed by Prusiner [29], while Dpl has been demonstrated to be not associated with the onset and development of these neurodegenerative diseases [10,36]. Doppel, similarly to the cellular prion protein, is in fact a GPI-anchored molecule but its expression is restricted to the plasma membrane of adluminal pole of human Sertoli cells and in correspondence of the flagella of mature ejaculated spermatozoa [28]; since Sertoli cells communicate with the germ ones either directly (cell–cell interaction) or indirectly (paracrine interaction) throughout gametogenesis, Dpl was proposed to be involved in spermiogenesis [28]; different authors have discovered that mice deficient for Dpl exhibited male sterility [5] and cellular models for Dpl functions in fertilization were suggested in mediating sperm–egg interaction [14]. On the other hand, other contributions have investigated Dpl cellular functions through protein-interaction studies. Unfortunately, these contributions did not address to clear physiological functions of Dpl, even considering different biological and cellular contexts [3,17]. Otherwise, we have investi-

*These authors contributed equally to the work.
**Corresponding author: Fax: +39 0382 528496; E-mail: sergio.c@ipvgen.unipv.it.

gated if Dpl might interact with some prion-interacting proteins, Grb2, GFAP and PrP itself, in astrocytoma cell line models, suggesting that Dpl was likely not involved in these protein partnerships [2]. Furthermore, during the past years, we have observed that the doppel encoding gene (*PRND*) was over-expressed in human astrocytic [11] and in haematological tumors [35]; additionally, *PRND* transcript was shown to be retained in the nucleus of the astrocytic tumor cells and its protein product was ectopically expressed in the cytoplasm of the neoplastic cells; additionally, Dpl was also hyper-glycosylated and it failed to be detected at the cell membranes [9].

Consequently, in this study we deeper investigated the unusual Dpl cellular localization in astrocytoma cell lines in order to gain a better understanding of some of the molecular events that accomplish the neoplastic cell transformation.

2. Material and methods

2.1. Cell lines

Human established glioblastoma cell lines IPDDC-A2 (ECACC, Salisbury, UK) and D384-MG (provided by Dr. Mauro Ceroni, University of Pavia, Italy) were used in the present study. IPDDC-A2 was derived from a Grade II mixed astrocytoma, while D384-MG is a clone isolated from a human glioblastoma (WHO grade IV) cell line, previously described [4]. IPDDC-A2 cells were cultivated in D-MEM medium supplemented with 10% FBS, 100 units/ml penicillin, 0.1 mg/ml streptomycin and 1% L-glutamine (GIBCO, Paisley, UK). D384-MG was maintained with D-MEM F12 medium (GIBCO) supplemented with 10% FBS, 100 units/ml penicillin, 0.1 mg/ml streptomycin and 1% L-glutamine.

Glioma (T98G and U373-MG) and human cervix tumor (HeLa) established cell lines were purchased from ECACC (UK). The human astrocytic tumor established PRT-HU2 cell line, previously described in [9] was isolated from a glioblastoma multiforme 61-years old female patient. These tumor cell lines were maintained in D-MEM medium supplemented with 10% FBS, 100 units/ml penicillin, 0.1 mg/ml streptomycin and 1% L-glutamine (GIBCO).

The tumor tissue for a glioma primary cell line was kindly provided by the Department of Neurosurgery, Monza (Italy), shortly after surgery of a 29-year-old male patient diagnosed with glioblastoma multiforme of the right temporal parietal lobe. Histological examination revealed a grade IV astrocytoma according to the WHO classification, and expressing GFAP immunohistochemically. The tumor tissue was washed with Hanks' balanced salt solution (HBSS; Sigma) and minced to 1–2 mm fragments with scissors. The fragments were dissociated by mechanical means and placed into 25 cm tissue culture flasks with D-MEM F12 supplemented 10% inactivated fetal calf serum (FBS) containing 100 units/ml penicillin and 0.1 mg/ml streptomycin. The culture was incubated at 37°C in a humidified atmosphere of 5% CO_2.

Normal human astrocytes (NHA) were purchased from Cambrex (UK) and cultivated in the specific astrocyte AGM medium (Cambrex) according to the manufacturer's specifications.

Glioma primary and NHA cells were maintained and fixed on coverslips at their second culture passages for immunofluorescent analysis.

2.2. Immunofluorescence microscopy

For immunofluorescence, different monoclonal and polyclonal antibodies were adopted. Species-specific Alexa Fluor 488 and Alexa Fluor 633 secondary conjugated antibodies (Invitrogen, Carlsbad, CA, USA) were coupled with primary antibodies and used as specified in Table 1. Cells cultured on coverslips were rinsed with phosphate-buffered saline (PBS), fixed immediately in 4% paraformaldehyde-PBS, pH 7.4, for 15 min at room temperature. Cells on coverslips were treated with 100 μl of Image-If Enhancer (Invitrogen) for 30 min at room temperature, according to the supplier's specifications. Cells were then incubated for 1 hour with primary antibodies diluted in PBS + 5% fat milk powder (w/v), using the dilutions reported in Table 1. Cells were washed with PBS and incubated for 1 hour with secondary antibodies (species-specific Alexa Fluor 488 or Alexa Fluor 633), diluted in PBS + 5% fat milk powder. Coverslips were then washed three times with PBS and treated with ProLong Gold antifade reagent with DAPI (Invitrogen) according to the manufacturer's instructions; finally, coverslips were mounted onto glass slides. Fluorescence was viewed using a fluorescence light inverted microscope (Nikon Eclipse TS100, Japan) with a 100× oil immersion objective. Confocal and Normanski interference contrast analysis were performed by laser scanning microscopy using a Leica TCS SPII microscopy equipped with the confocal inverted microscopy system Leica DM IRBE, using a 63× NA 1.32 oil immersion objective.

Table 1
Antibodies employed in immunofluorescence detection

Primary					Secondary		
Name	Target	Source	Provenience	Dil.	Name	Source	Dil.
H4A3	Lamp-1	Mouse monoclonal	Abcam	1:30	Alexa Fluor 488	Rabbit anti-mouse	1:100
G-20	Dpl	Goat polyclonal	Santa Cruz Biotechnologies	1:30	Alexa Fluor 633	Donkey anti-goat	1:100
N-18	Limp-2	Goat polyclonal	Santa Cruz Biotechnologies	1:30	Alexa Fluor 488	Donkey anti-goat	1:100
D7C7	Dpl	Mouse monoclonal	Dr. Man-Su Sy	1:30	Alexa Fluor 633	Rabbit anti-mouse	1:100
H4A3	Lamp-1	Mouse monoclonal	Abcam	1:30	Alexa Fluor 488	Rabbit anti-mouse	1:100
N-18	Limp-2	Goat polyclonal	Santa Cruz Biotechnologies	1:30	Alexa Fluor 633	Donkey anti-goat	1:100
RL90	PDI	Mouse monoclonal	Abcam	1:200	Alexa Fluor 488	Rabbit anti-mouse	1:200
G-20	Dpl	Goat polyclonal	Santa Cruz Biotechnologies	1:40	Alexa Fluor 633	Donkey anti-goat	1:200
CDF4	Golgin97	Mouse monoclonal	Invitrogen	1:30	Alexa Fluor 488	Rabbit anti-mouse	1:100
G-20	Dpl	Goat polyclonal	Santa Cruz Biotechnologies	1:30	Alexa Fluor 633	Donkey anti-goat	1:200
Ab1877	Catalase	Rabbit polyclonal	Abcam	1:100	Alexa Fluor 488	Donkey anti-goat	1:200
G-20	Dpl	Goat polyclonal	Santa Cruz Biotechnologies	1:30	Alexa Fluor 633	Donkey anti-goat	1:50

Antibodies were diluted (dil.) in PBS + 5% fat milk powder. Alexa Fluor 488 and 633 antibodies were provided by Invitrogen (USA).

2.3. Construction of wild-type and glycosylation mutant human Dpl expression plasmids

Both the *wild-type* and the glycosylation mutant Dpl proteins were cloned into two types of expression plasmids, containing or not-*EGFP*.

The non-fluorescent human *wild-type* Dpl expression vector, namely p-Dpl, was produced as follows: *PRND* coding sequence was amplified from 20 ng of human genomic DNA using Dpl-U and Dpl-L primers containing *XhoI* and *NotI* restriction sites (underlined), respectively: Dpl-U 5′-CCG CTC GAG CGG ATG AGG AAG CAC CTG AGC TG-3′ and Dpl-L 5′-ATT TGC GGC CGC TTA TTA TTT CAC CAT GAG CCA GAT CA-3′. After *XhoI/NotI* digestion, PCR products were cloned into the pEGFP-N1 expression plasmid (Clontech, Palo Alto, CA, USA), *XhoI/NotI* digested in order to delete *EGFP*.

The p-Dpl^{mut} vector, expressing Dpl with mutated glycosylation sites, was produced as follows. Mutagenesis was performed on p-Dpl to specifically introduce the threonine to alanine (at position 43) and asparagine to serine (at 98 and 110) substitutions into the amino acid sequence of Dpl, according to the QuickChange® mutagenesis kit guidelines (Stratagene, La Jolla, CA, USA). In particular, the following mutagenic primers (N98S-U, N98S-L; N110S-U, N110S-L; T43A-U, T43A-L) were adopted (mutated codons are underlined): N98S-U 5′-TGC TCT GAG GCT AGT GTG ACC AAG GAG GCA-3′ and N98S-L 5′-TGC CTC CTT GGT CAC ACT AGC CTC AGA GCA-3′, N110S-U 5′-TTT GTC ACC GGC TGC ATC AGT GCC ACC CAG G-3′ and N110S-L 5′-CCT GGG TGG CAC TGA TGC AGC CGG TGA CAA A-3′, O43A-U 5′-AAG GCC CTG CCC AGC GCT GCC CAG ATC ACT-3′ and O43A-L 5′-AGT GAT CTG GGC AGC GCT GGG CAG GGC CTT-3′. To obtain p-Dpl^{mut}, three serial mutagenesis experiments were performed. For each mutagenesis step a long PCR was performed as follows: 50 μl reaction containing 20 ng of p-Dpl plasmid, 100 ng of each primer, 0.2 mM dNTPs, 2.5 U of AccuTaq™ LA DNA Polymerase (Sigma, St. Louis, MO, USA) was amplified for 18 cycles consisting of 30 s denaturation at 95°C, 1 min annealing step at 60°C, followed by a 6 min extension step at 68°C. After PCR-based site-specific mutagenesis, the plasmid was digested with *Dpn*I and transformed into *E. coli* DH5α competent cells. Colonies were screened by PCR and the positive clones were sequenced.

The *EGFP*-fluorescent human *wild-type* Dpl construct, namely pEGFP-N1/Dpl, was made as described in Comincini et al. [9]. Briefly, the pEGFP-N1 plasmid (Clontech) was mutagenized by PCR using the primers 5′-CCG GAA TTC CCA CCA TGG TGA GCA AGG GCG AG-3′ and 5′-GTC GCG GCC GCT TTC TTG TAC AGC TCG TCC ATG-3′, to remove the stop codon at the end of *EGFP*. The pEGFP-N1/Dpl construct was produced amplifying the *PRND* amino terminal signal peptide coding region (from 1 to 25 Dpl residues) with the primers 5′-CCG CTC GAG CGG ATG AGG AAG CAC CTC AGC TG-3′ and 5′-CCG AAT TCG CTG GAC CGC AGA GAG GT-3′. This *PRND* portion was then cloned into the pEGFP-N1 mutagenized plasmid, 5′ of *EGFP,* in the *Xho*I

and *Eco*RI restriction sites. The remaining *PRND* peptide coding region (26–176 Dpl residues) was amplified using the primers 5′-GCG GCC GCT ACG AGG GGC ATC AAG CAC A-3′ and 5′-TGC GGC CGC TTA TTT CAC CAT GAG CCA GAT CA-3′. The product was then cloned downstream of *EGFP* in the modified pEGFP-N1 plasmid, using the *Not*I restriction site, thus obtaining pEGFP-N1/Dpl. The pEGFP-N1/Dpl^{mut}, expressing the Dpl protein with mutated glycosylation sites, was obtained amplifying the Dpl 26–176 peptide coding region from p-Dpl^{mut}, using the primers 5′-GCG GCC GCT ACG AGG GGC ATC AAG CAC A-3′ and 5′-TGC GGC CGC TTA TTT CAC CAT GAG CCA GAT CA-3′, and cloning the *Not*I digested PCR purified product into the mutagenized pEGFP-N1 plasmid. Each construct, i.e. p-Dpl and p-Dpl^{mut}, pEGFP-N1/Dpl and pEGFP-N1/Dpl^{mut} were confirmed by DNA sequencing.

2.4. Astrocytoma cells transfections and immunofluorescence

Highly purified p-Dpl or p-Dpl^{mut}, pEGFP-N1/Dpl or pEGFP-N1/Dpl^{mut} plasmids (1 μg) were mixed with 0.1 ml of transfection medium (D-MEM supplemented with 10% FBS and 1% L-glutamine). The mixture was incubated at room temperature for 5 min. Then, 2.5 μl of Lipofectamine 2000 reagent (Invitrogen) was added to the mixture, mixed for 10 s and finally incubated at room temperature for 20 min. IPDDC-A2 and D384-MG cells (plated one day before transfection at 5×10^5 into 30 mm culture dishes) were washed with PBS and trypsinized before adding the transfection mixture. The cells were then plated on glass coverslips and incubated for additional 24 h at 37°C and 5% CO_2. Dpl protein was visualised using anti-Dpl goat polyclonal G-20 (Santa Cruz Biotechnology, Santa Cruz, CA, USA) and Alexa Fluor 488 (Invitrogen) antibodies, as indicated in Table 1, by means of confocal and Normanski interference contrast microscopic examinations, as previously described.

2.5. Lysosomal pathway investigations

IPDDC-A2 and D384-MG astrocytoma cell lines (1.5×10^5 cells) were seeded onto coverslips glasses the day before the treatment, as above described. The cells were then treated with 10 mM ammonium chloride (Sigma) and incubated for 24–48–72 h in culture medium. After each treatment, the cells were fixed in 4% paraformaldehyde-PBS (pH 7.4) and incubated with G-20 anti-Dpl and Alexa Fluor 488 donkey anti-goat antibodies, as indicated in Table 1. Immunofluorescence was performed using DIC interference contrast microscopic examinations.

2.6. Western blot analysis

For immunoblot analysis of IPDDC-A2 and D384-MG cell extracts, 50 μg of total protein lysates were quantified using the Qubit instrument, according to the Quant-iT Protein Assay kit (Invitrogen), boiled for 5 min in Laemmli sample buffer (2% SDS (w/v), 6% Glycerol (v/v), 150 mM β-mercaptoethanol, 0.2% bromophenol blue (w/v), 62.5 mM Tris–HCl pH 6.8) and electrophoresed by SDS-PAGE (12% gel). Proteins were transferred onto a nitro-cellulose membrane Hybond™-C Extra (Amersham Biosciences, Little Chalfont, Buckinghamshire, UK). Membranes were blocked with 2% non-fat milk in PBS containing 0.1% Tween™ 20. The primary and secondary antibodies (Table 1) employed for immunodetection were used at 1:10000 dilution. As a control, an anti-GAPDH mouse monoclonal antibody (Ambion) was adopted at 1:20000. Blots were treated with specific peroxidase-coupled secondary antibodies (1:10000 dilution) and protein signals were revealed by the "ECL Advance™ Western Blotting Detection Kit" (Amersham Biosciences).

3. Results

Previous studies showed that Dpl was over-expressed in glioma specimens [11] and in astrocytoma cell lines [9]. In these studies, Dpl showed a diffuse and granular staining, suggesting a cytoplasmic accumulation of the protein within glial tumor cells.

In the present study, confocal microscopy was used to examine in further detail the Dpl sub-cellular localization in astrocytomas. We have therefore performed immunofluorescence localization of Dpl in two established tumor astrocytic cell lines, namely IPDDC-A2 and D384-MG, using different anti-Dpl and organelle-specific antibodies, reported in Table 1. Generally, these astrocytoma cells predominantly exhibited overlapping multi-punctate patterns of Dpl cytoplasmic localization, suggesting the presence of protein aggregates. These Dpl mass-like conglomerates were mainly identified in peri-nuclear proximal regions. Differently, no Dpl signal was highlighted in correspondence of the cellular membranes (Fig. 1, panels c

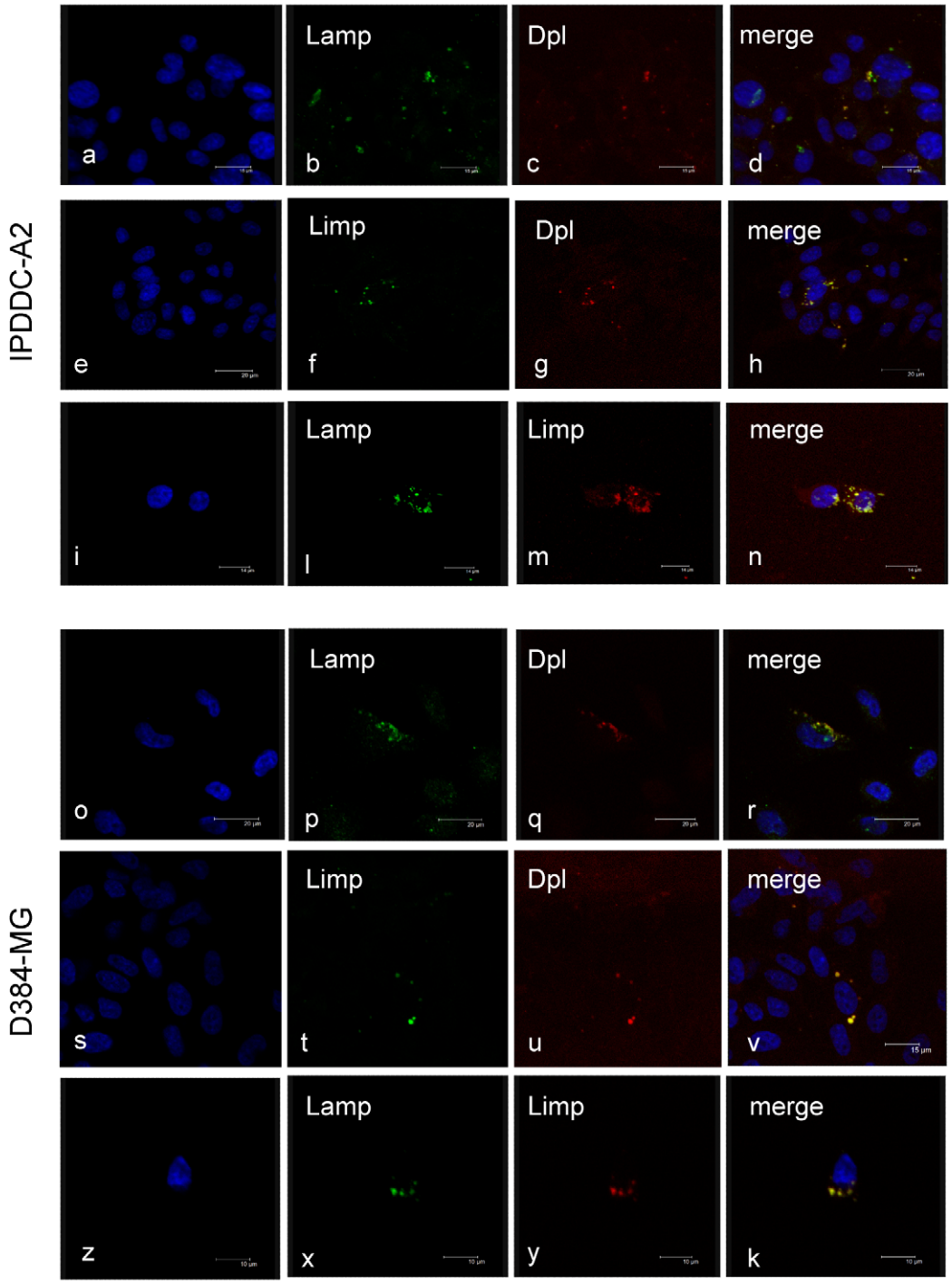

Fig. 1. Sub-cellular localization of Dpl in IPDDC-A2 and D384-MG astrocytoma cells. Cells were grown on glass slides as described in Materials and methods. At 48 hours, cells were fixed and incubated with primary antibodies, specifically mouse monoclonal Lamp-1 (Abcam) and G-20 (Santa Cruz Biotechnologies), anti-Dpl goat polyclonal or goat polyclonal Limp-2 (Santa Cruz Biotechnologies) and mouse monoclonal D7C7 antibodies. Species-specific Alexa Fluor 488 and Alexa Fluor 633 secondary antibodies (Invitrogen) were finally employed, as illustrated in Table 1. Panels i–n (IPDDC-A2) and z–k (D384-MG) indicated co-localization of the lysosomal membrane protein markers, i.e. Lamp-1 and Limp-2. Slides were incubated with ProLong Gold antifade reagent with DAPI (Invitrogen) to stain nuclei (blue). The cell morphology and fluorescence were observed with a confocal fluorescence microscope (Leica, original magnification, 63×). The scale bars are reported.

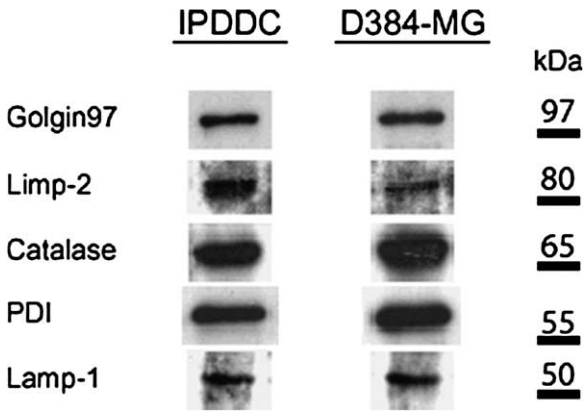

Fig. 2. Expression of organelle specific markers in IPDDC-A2 and D384-MG cells. Immunoblotting of Lamp-1 and Limp-2 for lysosomes, PDI for ER, Golgin97 for Golgi and Catalase for peroxisomes, was produced using the antibodies described in Table 1. Molecular weights, in kDa, was reported. Immunodetection was performed on the following amount of total extracted proteins: Golgin97 (20 μg), Limp-2, Lamp-1 and Catalase (50 μg) and PDI (2.5 μg).

and g for IPDDC-A2; q and u for D384-MG cells). Consequently, a panel of organelle specific markers, namely Lamp-1 and Limp-2 for lysosomes, PDI for ER, Golgin97 for Golgi and Catalase for peroxisomes, were employed for Dpl co-localization: the endogenous expression of the markers was primary assayed by Western blot in IPDDC-A2 and D384-MG cell lysates (Fig. 2). In these cells, Dpl was extensively co-localized with lysosomal membrane proteins, Lamp-1 and Limp-2, demonstrated by the yellow patches in the merged images (Fig. 1, panels d, h, r, v); additionally, Lamp-1 and Limp-2 showed nearly identical localization signals in the investigated cells (Fig. 1, panels n, k). Similar results in Dpl-lysosome co-localization were obtained using different monoclonal (D7C7) and polyclonal (DplVal, N-20 and FL176) anti-Dpl antibodies, as well as adopting additional astrocytoma cell lines (T98G, PRT-HU2 and U373-MG); differently, a predominant nuclear Dpl immunoreactivity was detected in the U87-MG astrocytoma cell line (data not shown).

Furthermore, differently from lysosomes, Dpl was barely detected in the other organelles, with the majority of the signals in correspondence of the Golgi apparatus (data available upon request). At last, co-immunoprecipitation experiments failed to detect Dpl–Limp 2 or Dpl–Lamp 1 interactions.

Dpl endogenous expression was investigated in a primary glioma cell line, isolated from a WHO IV patient and in normal human astrocytes (NHA): as reported in Fig. 3, Dpl was expressed in the primary glioma cells (panel a), with, however, a lesser extent of lysosome co-localization signals (c) compared to continuous glioma cell lines; differently, Dpl has a very faint expression in few NHA cells, with punctuate signals in the cytoplasm (d) and absence of Dpl-lysosome co-localization (f).

As previously reported, Dpl exhibited abnormal glycosylation patterns in several astrocytoma cell lines, including the investigated IPDDC-A2 and D384-MG ones [9]. In order to address if such abnormal post-translational modifications might influence the topology of Dpl in astrocytoma cells, we have therefore constructed a Dpl expression mutagenized plasmid (p-Dpl^{mut}), specifically in correspondence of O-(Thr 43) and N-glycosylation (Asn 98 and Asn 110) sites. Through site specific mutagenesis, these positions were substituted by the amino acids alanine (at position 43) and serine (98 and 110). Similarly, a chimaeric mutagenized Dpl vector (pEGFP-N1/Dpl^{mut}) expressing *EGFP* was constructed. As controls, *wild-type* Dpl expression vector, i.e. p-Dpl, and pEGFP-N1/Dpl vector expressing both Dpl and EGFP, were produced (see Section 2). These plasmids were sequenced, transfected and transiently expressed in IPDDC-A2 and D384-MG cells. Then, the cells were subjected to immunofluorescence reactions, followed by confocal and Normanski contrast interference microscopy examinations, using G-20 goat polyclonal anti-Dpl primary antibody and followed by incubation with Alexa Fluor 488 secondary antibody (Table 1). The results, reported in Fig. 4, indicated that p-Dpl and pEGFP-N1/Dpl expression gave cytoplasmic immunoreactive signals, similar to the endogenous Dpl ones (panels a and b in IPDDC-A2; f and g in D384-MG cells); differently, Dpl-membrane localization signals were shown in few cells after p-Dpl^{mut} expression (c, d; h, i). Similar membrane staining were obtained using the pEGFP-N1/Dpl^{mut} mutated plasmid (e, l). Western blot analysis after the isolation of membrane and whole total proteins of IPDDC-A2 and D384-MG cells, transfected with p-Dpl^{mut} vector, failed to reveal differences in Dpl expression compared to non-transfected cells. On the contrary, HeLa transfected cells with the p-Dpl^{mut} vector highlighted a Dpl unglycosylated band at 17–18 kDa by Western blot analysis (data not shown).

To further investigate on the Dpl lysosomal localization in the astrocytoma, IPDDC-A2 and D384-MG cells were treated with ammonium chloride, a known lysosomal inhibitor. The cells at different densities (from 10^4 to 1.5×10^5 cells, cultivated onto stan-

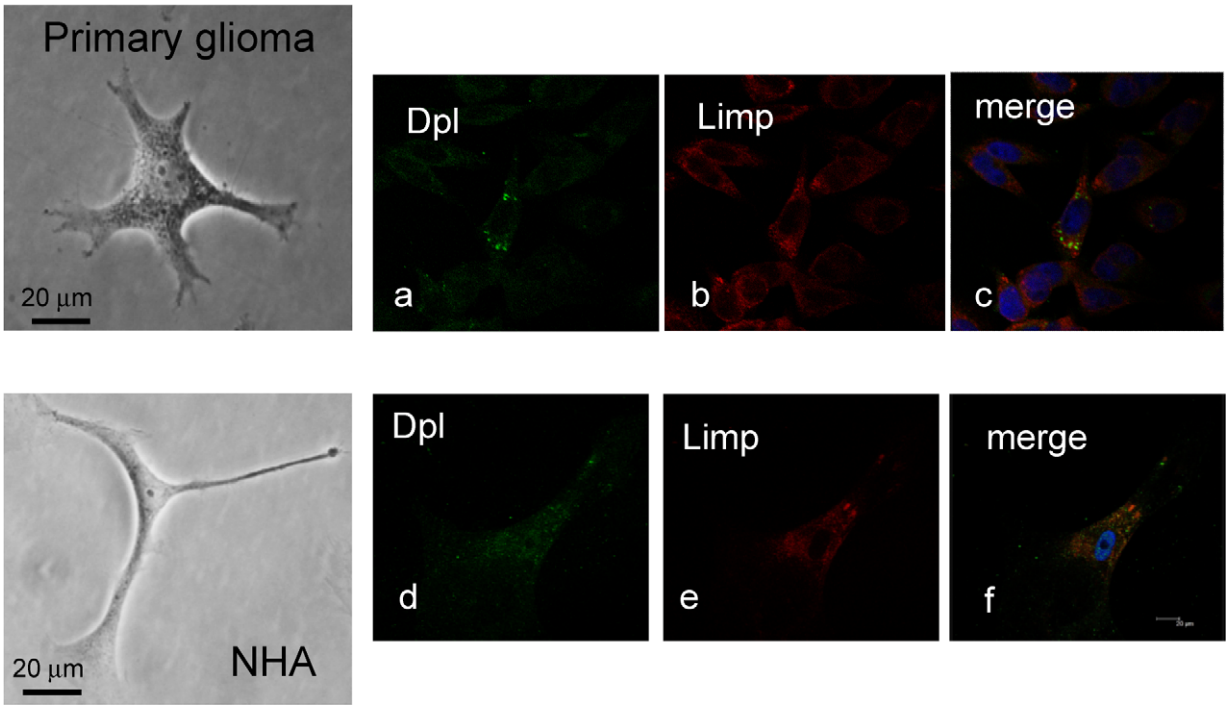

Fig. 3. Dpl expression in a primary glioma and in normal human astrocytic cells. At their second culture-passages, cells were fixed and incubated with primary antibodies, specifically goat polyclonal Limp-2 (Abcam) and mouse monoclonal anti-Dpl D7C7 antibodies. Species-specific Alexa Fluor 488 and Alexa Fluor 633 secondary antibodies (Invitrogen) were employed, as illustrated in Table 1. Slides were incubated with ProLong Gold antifade reagent with DAPI (Invitrogen) to stain nuclei (blue). The cell morphology and fluorescence were observed with a confocal fluorescence microscope (Leica, original magnification, 63×). The scale bars are reported.

dard microscopic glass coverslips) were subjected to different concentrations of the inhibitor (10–30 mM) and their viability was evaluated through microscopic examinations. In particular, using high concentration of ammonium chloride (30 mM), a high percentage (about 80%) of cells death was reported. Therefore, to investigate the effect of the lysosomal inhibition on the Dpl expression, we adopted a low concentration of ammonium chloride (10 mM) in presence of a high density of cells (1.5×10^5 cells *per* coverslip). Generally, after 48 hours of the treatment, a cytoplasmic increase of vacuolization compared to the control was observed (Fig. 5, panels a and b for IPDDC-A2; g and h for D384-MG cells, respectively); finally, at 72 hours the cells exhibited difference in morphology with large budding vesicles that de-touched from the plasma membrane (c, i). Dpl immunofluorescence studies showed after 48 hours a more diffuse cytoplasmic localization, and, additionally, some cells showed an intense staining in correspondence of the inner plasma membranes (d, l); noticeably, the Dpl staining in the vesicles significantly increased after 72 hours of the treatment, even through the release of Dpl-positive exocytic vesicles in the medium (e, f; m, n). Following this treatment, immunoblotting analysis was employed to investigate Dpl expression in IPDDC-A2 and D384-MG cells. As reported in Fig. 5, comparing to the untreated samples, a significant increase in Dpl expression was observed in IPDDC-A2 cells after 48 and 72 hours p.t., while a lesser variation in Dpl expression was observed in D384-MG cells.

4. Discussion

Recently, a novel protein, named doppel (Dpl), was identified which shares significant biochemical and structural homology with PrP^C [25,33]. Differently from PrP^C, Dpl is dispensable for prion diseases progression, but Dpl appears to have an essential function in male spermatogenesis (reviewed in [6]). Doppel gene (*PRND*) expression is highly tissue-specific and developmental stage-dependent, normally quiescent in adult brain but highly active in testis. However, abnormal and high levels of Dpl protein has been observed in human astrocytoma and in other non-glial tu-

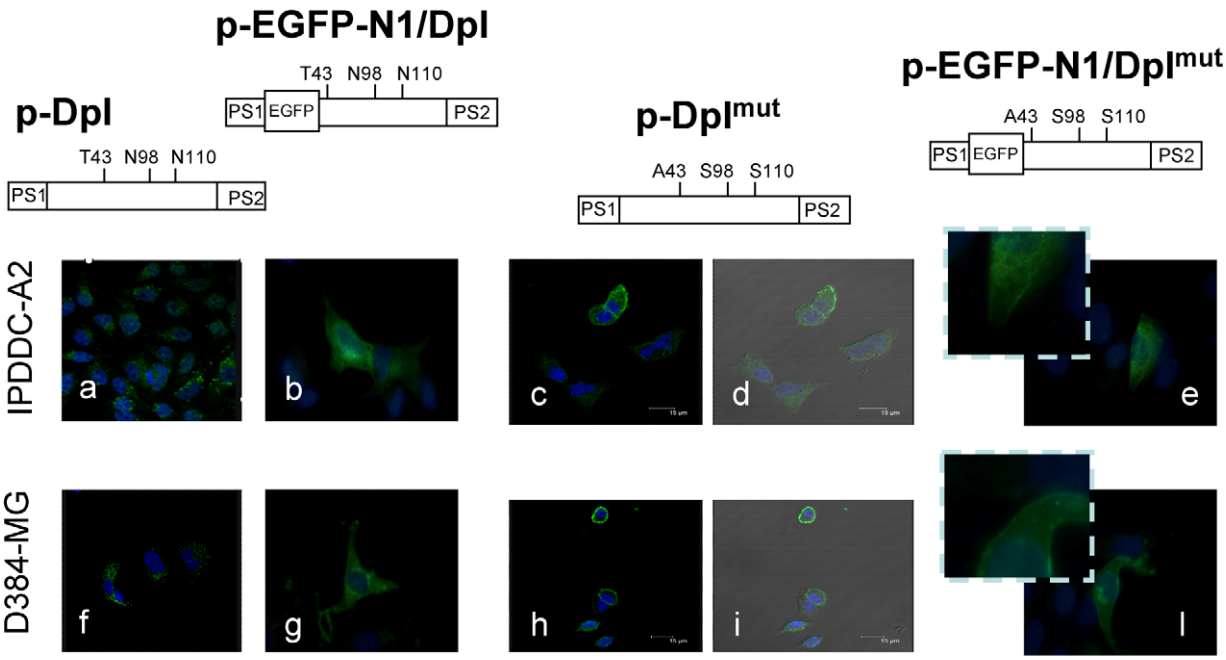

Fig. 4. Dpl transfection in astrocytoma cells. IPDDC-A2 and D384-MG cells (5×10^5 onto 30 mm dishes) were transfected with 1 µg of p-Dpl, pEGFP-N1/Dpl, p-Dpl^{mut} or pEGFP-N1/Dpl^{mut} expression vectors, combined with 2.5 µl of Lipofectamine 2000 (Invitrogen) as a transfection agent. After 24 hours post-transfection the medium was changed and the following day the cells were fixed on glass slides. Single immunofluorescence reactions were performed using G-20 anti-Dpl goat polyclonal (Santa Cruz Biotechnologies) and Alexa Fluor 488 (Invitrogen) antibodies. In pEGFP-N1/Dpl and pEGFP-N1/Dpl^{mut} transfected cells, EGFP was excited at 488 nm wavelength. IPDDC-A2 and D384-MG cells showed a diffuse cytoplasmic Dpl expression after p-Dpl and pEGFP-N1/Dpl transfection (respectively, panels a, b; f, g) while a plasma membrane Dpl localization was highlighted in p-Dpl^{mut} and pEGFP-N1/Dpl^{mut} transfected cells, after confocal or Normanski interference contrast examinations (c, d, e; h, i, l). Cells were visualized with a confocal fluorescence microscope (Leica, original magnification, 63×). The scale bars are reported.

mor specimens [8]. These findings suggest that *PRND* is activated under tumorigenic conditions that might be associated with the tumor progression [8]. In the astrocytic tumors that we have recently studied, Dpl is ectopically expressed in the cell cytoplasm [9]. In this context we have therefore deeper investigated the sub-cellular localization of Dpl in astrocytoma, reporting that Dpl-positive signals were localized in the lysosomes, through immunoreactivity to Limp-2 and Lamp-1 lysosome specific markers.

Lysosomes are acidic membrane-bound organelles involved in degradation of extracellular materials internalized by endocytosis and intracellular materials derived from autophagic processes [12,18]. The formation of lysosomes requires protein transport from the biosynthetic and the endocytic pathway. Proteins destined to be targeted to lysosomes are delivered to an acidic endosomal compartment either from the trans-Golgi network or from the plasma membrane via endocytosis. This system therefore contributes to the maintenance of homeostasis via numerous functions, including the supply of nutrients, the turnover of cellular proteins, the elimination of defective or unfavourable molecules and the down-regulation of surface receptors [37].

The sub-cellular localization of Dpl observed in astrocytoma cells (this study) is markedly different from the Dpl outer membrane attachment to neuro-2a (N2a) cells through its GPI anchor, as previously reported [33]. Furthermore, Massimino and colleagues [24] expressed human Dpl and PrP^C in neuroblastoma cells and demonstrated that the two proteins co-patched extensively at the cell membrane; additionally, when the two proteins were internalized by cross-linking to the cholera toxin, Dpl and PrP^C were together endocytosed within the Golgi complex [24]. Differently, our results pointed that Dpl was not detected on the cell membranes and that its internalization pathway is different from that previously described in neuroblastoma cells; in fact, Dpl is barely detected in both Golgi and ER apparatus, showing a predominant accumulation within lysosomal vesicles. The most parsimonious explanation to this observation might be that the tumor cells may overproduce Dpl and its internalization into

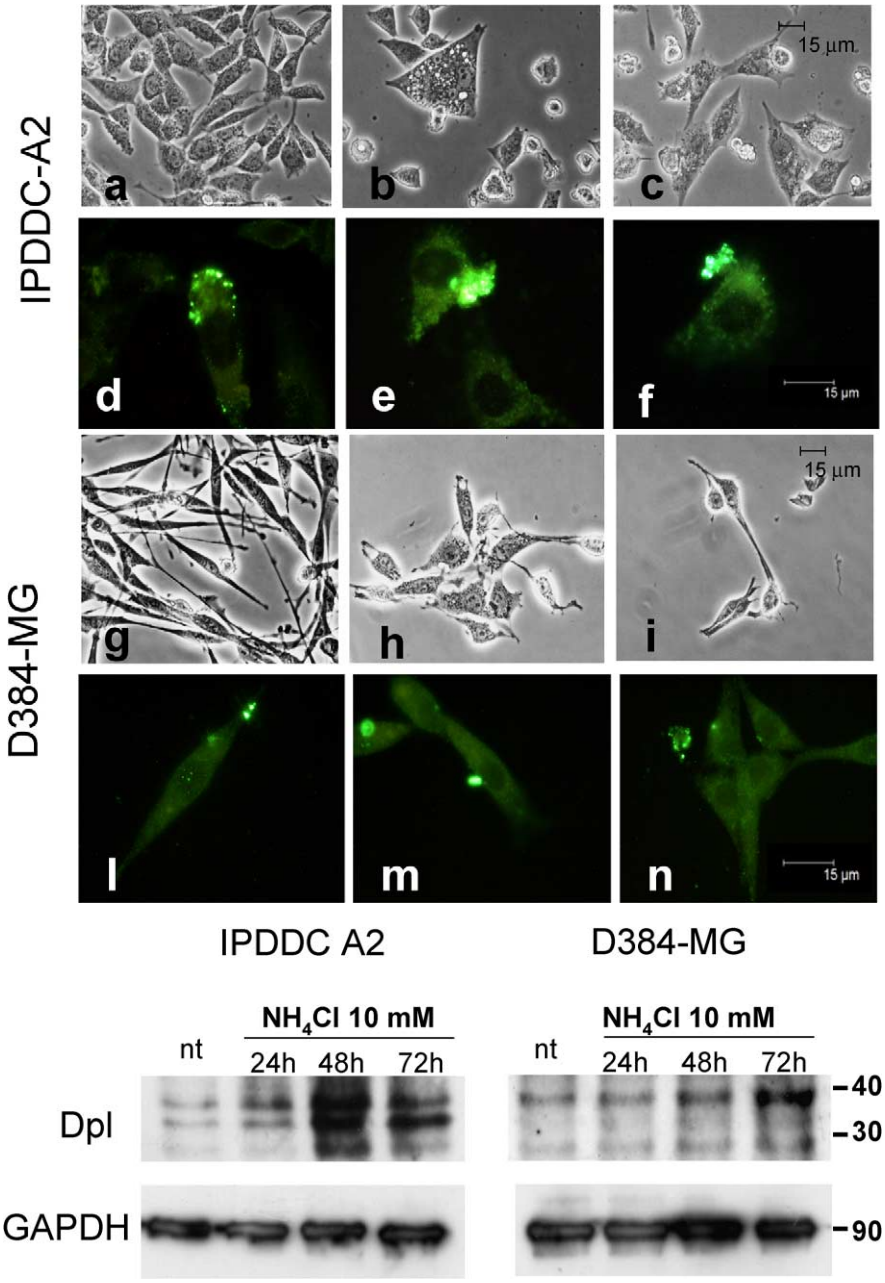

Fig. 5. Effect of ammonium chloride treatment on the Dpl traffic and expression in IPDDC-A2 and D384-MG cells. IPDDC-A2 cells were treated with 10 mM ammonium chloride, analysed in their morphology and in Dpl immunofluorescence after 24, 48 and 72 h, and finally compared to untreated control cells (a); extensive vacuolization was observed at 48 h (b) and several budding vesicles after 72 h (c). Dpl immunolocalization showed strong signals after 48 h in correspondence of the inner layer of the plasma membrane (d); Dpl was significantly accumulated in nascent budding and exocytic vesicles at 72 h (e and f). In D384-MG cells, treated as above, changes in morphology compared to the controls (g) were observed after 48 h (h), while several rounded and shrunken cells appeared after 72 h (i). Dpl immunolocalization showed strong signals after 48 hours in correspondence of the apical portion of the cells (l); as above described, Dpl was significantly accumulated in nascent budding and exocytic vesicles at 72 h (m and n). The morphology of the cells and Dpl immunofluorescence reactivity were DIC visualised with an inverted fluorescence microscope (Eclipse TS100, Nikon, original magnifications, 10, 40 and 100×). The scale bars are reported. Dpl expression in IPDDC-A2 and D384-MG cells was analysed by immunoblotting using the D7C7 anti-Dpl monoclonal antibody. Controls (NT) were compared to ammonium chloride treated cells after 24, 48 and 72 h. Control GAPDH protein expression was reported. Molecular weights (kDa) are indicated.

lysosomes could serve to eliminate the excess of protein. This concept could be reinforced by the fact that Dpl has a cellular toxic effect that could be directly counteracted by the expression of PrP^C and possibly through a direct interaction of the two proteins [32]. In a different cellular context, i.e. healthy adult rat astrocytes, Dpl shared co-localization with PrP^C on cell membrane: additionally, Dpl was shown to directly interact with PrP^C [30]. These differences in Dpl localization between tumoral glial and nervous cells might reflect a complex recycling machinery of the astrocytomas membrane proteins where GPI-linked proteins have remarkably different traffic and half-life within the cells, as previously reported [21,22].

In astrocytic tumor cells, Dpl is a highly glycosylated protein and it is ectopically expressed in the cell cytoplasm, as we previously reported [9]. We have therefore investigated if glycosylation *per se* could be involved in differences in the topology of Dpl in these glial tumor cells. As highlighted in the microscopic examination of p-Dpl^{mut} and pEGFP–N1/Dpl^{mut} transfected cells, the absence of glycosylation sites targeted Dpl to the membrane of a limited number of astrocytoma cells. Additionally, Normanski interference contrast examinations showed that some Dpl-membrane positive transfected cells became round and shrunken. Due to the limited number of the Dpl-membrane positive cells, Western blot failed to reveal differences in Dpl expression. Differently, immunoblotting analysis of protein lysates from HeLa transfected cells with the mutated Dpl expression vector p-Dpl^{mut} evidenced a band of 17–18 kDa, likely represented by the unglycosylated Dpl isoform (data not shown).

As a comment of our results, glycosylation might therefore be involved in the traffic and in the cytoplasmic localization of the Dpl protein in astrocytic tumor cells: our experiments indicated that a plasma membrane localization of Dpl needs at least post-translational modifications of the protein and that this cellular localization seems not well efficient and tolerated by the tumor cells. In fact, it is known that protein linked oligosaccharide moieties are considered to serve diverse functions. They stabilize the proteins against denaturation and proteolysis, enhance solubility, modulate immune responses, facilitate orientation of proteins relative to a membrane, confer structural rigidity to proteins and regulate their turnover [16]. Furthermore, it has long been predicted that the carbohydrate moieties of glycoproteins play important roles in the physical function and structural stability of the cell surface proteins [15].

According to our results, the most parsimonious explanation of Dpl localization in lysosomes, could be that the excess of a potentially cytotoxic Dpl product was targeted to these organelles for degradation. We therefore interfered with the lysosomal degradation pathway, treating the astrocytoma cells with ammonium chloride, a known lysosomotropic compound, resulting in alkalinization of the acidic compartments [26]. Our results suggest that the lysosomal compartments may be important for the cellular traffic and the expression of Dpl in astrocytoma cells: the raising of the pH of lysosomes by means of ammonium chloride might contribute to the mis-sorting of Dpl and its accumulation within the cells and finally in the exocytic vesicles. Additionally, as previously reported, the defective acidification of intracellular organelles in cancer cells results in aberrant secretion of different cytoplasmic proteins [19]. Nevertheless, we cannot exclude the possibility that the delivery of Dpl to lysosomes serves additional functions apart from those discussed. In particular, the absence of expression or the rapid turnover of some membrane proteins within astrocytoma cells might also contribute to a complex reassortment of plasma membrane proteins likely plausible in such cancers [1]. Further studies on the alteration of the traffic of plasma membrane proteins in cancer cells – as documented for Dpl in this study – should be required to increase our knowledge on the molecular processes involved in malignant cell transformation.

Acknowledgements

This work was supported by a grant from the Italian Ministry for Education, University and Research (MIUR), “Progetti di Ricerca di Interesse Nazionale (2005)”. A.A. is granted by “Fondo Sociale Europeo”. The authors are grateful to Dr. Patrizia Vaghi (Centro Grandi Strumenti, University of Pavia, Italy) for technical support in confocal microscopy examinations, to Prof. Giovanna Valentini (University of Pavia) and Dr. Man-Sun Sy (Case Western Reserve University, USA) for providing DplVal and D7C7 anti-Dpl antibodies, respectively.

References

[1] M.M. Aloysius, R.A. Robins, J.M. Eremin et al., Vaccination therapy in malignant disease, *Surgeon* **4** (2006), 309–320.

[2] A. Azzalin, I. Del Vecchio, L.R. Chiarelli et al., Absence of interaction between doppel and GFAP, Grb2, PrPc proteins in human tumor astrocytic cells, *Anticancer Res.* **25** (2005), 4369–4374.

[3] A. Azzalin, I. Del Vecchio, L. Ferretti and S. Comincini, The prion-like protein Doppel (Dpl) interacts with the human receptor for activated C-kinase 1 (RACK1) protein, *Anticancer Res.* **26** (2006), 4539–4547.

[4] A.J. Balmfort, S.G. Ball, R.I. Freshney et al., D-1 dopaminergic and b-adrenergic stimulation of adenylate cyclase in a clone derived from the human astrocytoma cell line G-CCM, *J. Neurochem.* **47** (1986), 715–719.

[5] A. Behrens, N. Genoud, H. Naumann et al., Absence of the prion protein homologue Doppel causes male sterility, *EMBO J.* **21** (2002), 3652–3658.

[6] A. Behrens, Physiological and pathological functions of the prion protein homologue Dpl, *Br. Med. Bull.* **66** (2003), 35–42.

[7] S. Comincini, M.G. Foti, M.A. Tranusis et al., Genomic organization, comparative analysis, and genetic polymorphisms of the bovine and ovine prion Doppel genes (PRND), *Mamm. Genome* **12** (2001), 729–733.

[8] S. Comincini, A. Facoetti, I. Del Vecchio et al., Differential expression of the prion-like protein doppel gene (PRND) in astrocytomas: a new molecular marker potentially involved in tumor progression, *Anticancer Res.* **24** (2004), 1507–1517.

[9] S. Comincini, L.R. Chiarelli, P. Zelini et al., Nuclear mRNA retention and aberrant doppel protein expression in human astrocytic tumor cells, *Oncol. Rep.* **16** (2006), 1325–1332.

[10] S. Comincini, I. Del Vecchio and A. Azzalin, The doppel gene biology: a scientific journey from brain to testis, and return, *Centr. Eur. J. Biol.* **1** (2006), 494–505.

[11] S. Comincini, V. Ferrara, A. Arias et al., Diagnostic value of PRND gene expression profiles in astrocytomas: relationship to tumor grades of malignancy, *Oncol. Rep.* **17** (2007), 989–996.

[12] C. de Duve, Lysosomes revisited, *Eur. J. Biochem.* **137** (1983), 391–397.

[13] A. Espenes, I. Harbitz, S. Skogtvedt et al., Dynamic expression of the prion-like protein Doppel in ovine testicular tissue, *Int. J. Androl.* **29** (2006), 400–408.

[14] N. Genoud, A. Behrens, I. Arrighi et al., Prion proteins and infertility: insight from mouse models, *Cytogenet. Genome Res.* **103** (2003), 285–289.

[15] R.S. Haltiwanger and J.B. Lowe, Role of glycosylation in development, *Ann. Rev. Biochem.* **73** (2004), 491–537.

[16] A. Helenius and M. Aebi, Roles of N-linked glycans in the endoplasmic reticulum, *Ann. Rev. Biochem.* **73** (2004), 1019–1049.

[17] C. Hundt and S. Weiss, The prion-like protein Doppel fails to interact with itself, the prion protein and the 37 kDa/67 kDa laminin receptor in the yeast two-hybrid system, *Biochim. Biophys. Acta* **1689** (2004), 1–5.

[18] W. Hunziker and H.J. Geuze, Intracellular trafficking of lysosomal membrane proteins, *Bioessays* **18** (1996), 379–389.

[19] N. Kokkonen, A. Rivinoja, A. Kauppila et al., Defective acidification of intracellular organelles results in aberrant secretion of cathepsin D in cancer cells, *J. Biol. Chem.* **279** (2004), 39982–39988.

[20] S. Kornfeld and I. Mellman, The biogenesis of lysosomes, *Ann. Rev. Cell. Biol.* **5** (1989), 483–525.

[21] P. Lemansky, S.H. Fatemi, B. Gorican et al., Dynamics and longevity of the glycolipid-anchored membrane protein, Thy-1, *J. Cell Biol.* **110** (1990), 1525–1531.

[22] N. Madore, K.L. Smith, C.H. Graham et al., Functionally different GPI proteins are organized in different domains on the neuronal surface, *EMBO J.* **18** (1999), 6917–6926.

[23] E. Makrinou, J. Collinge and M. Antoniou, Genomic characterization of the human prion protein (PrP) gene locus, *Mamm. Genome* **13** (2002), 696–703.

[24] M.L. Massimino, C. Ballarin, A. Bertoli et al., Human Doppel and prion protein share common membrane microdomains and internalization pathways, *Int. J. Biochem. Cell Biol.* **36** (2004), 2016–2031.

[25] R.C. Moore, I.Y. Lee, G.L. Silverman et al., Ataxia in prion protein (PrP)-deficient mice is associated with upregulation of the novel PrP-like protein doppel, *J. Mol. Biol.* **292** (1999), 797–817.

[26] C.R. Morales, Q. Zhao and S. Lefrancoise, Biogenesis of the lysosomes by endocytic flow of plasma membrane, *Biocell* **23** (1999), 149–160.

[27] D. Paisley, S. Banks, J. Selfridge et al., Male infertility and DNA damage in Doppel knockout and prion protein/Doppel double-knockout mice, *Am. J. Pathol.* **164** (2004), 2279–2288.

[28] K. Peoc'h, C. Serres, Y. Frobert et al., The human "prion-like" protein Doppel is expressed in both Sertoli cells and spermatozoa, *J. Biol. Chem.* **277** (2002), 43071–43078.

[29] S.B. Prusiner, Novel proteinaceous infectious particles cause scrapie, *Science* **216** (1982), 136–144.

[30] K. Qin, L. Zhao, Y. Tang et al., Doppel-induced apoptosis and counteraction by cellular prion protein in neuroblastoma and astrocytes, *Neuroscience* **141** (2006), 1375–1388.

[31] M. Rondena, F. Ceciliani, S. Comazzi et al., Identification of bovine doppel protein in testis, ovary and ejaculated spermatozoa, *Theriogenology* **63** (2005), 1195–1206.

[32] D. Rossi, A. Cozzio, E. Flechsig et al., Onset of ataxia and Purkinje cell loss in PrP null mice inversely correlated with Dpl level in brain, *EMBO J.* **20** (2001), 694–702.

[33] G.L. Silverman, K. Qin, R.C. Moore et al., Doppel is an N-glycosylated, glycosylphosphatidylinositol-anchored protein, *J. Biol. Chem.* **275** (2000), 26834–26841.

[34] M.A. Tranulis, A. Espenes, S. Comincini et al., The PrP-like protein Doppel gene in sheep and cattle: cDNA sequence and expression, *Mamm. Genome* **12** (2001), 376–379.

[35] E. Travaglino, S. Comincini, C. Benatti et al., Overexpression of the Doppel protein in acute myeloid leukaemias and myelodysplastic syndromes, *Br. J. Haematol.* **128** (2005), 877–884.

[36] N.L. Tuzi, E. Gall, D. Melton et al., Expression of doppel in the CNS of mice does not modulate transmissible spongiform encephalopathy disease, *J. Gen. Virol.* **83** (2002), 705–711.

[37] A. Vellodi, Lysosomal storage disorders, *Br. J. Haematol.* **128** (2004), 413–431.